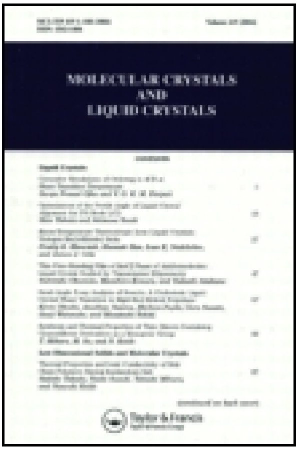

Molecular Crystals and Liquid Crystals
Publication details, including instructions for authors and subscription information:
http://www.tandfonline.com/loi/gmcl16

Two Frequency Addressing of a DTN-Cell

I. Fukuda [a b], M. Akatsuka [a c], T. Uchida [a] & M. Wada [a]

[a] Department of Electronic Engineering, Faculty of Engineering, Tohoku University, Sendai, 980, Japan

[b] Kanazawa Institute of Technology, Kanazawa, 921, Japan

[c] Asahi Glass Coroportion Ltd., Yokohama, 221, Japan

Version of record first published: 14 Oct 2011.

To cite this article: I. Fukuda, M. Akatsuka, T. Uchida & M. Wada (1981): Two Frequency Addressing of a DTN-Cell, Molecular Crystals and Liquid Crystals, 68:1, 311-330

To link to this article: http://dx.doi.org/10.1080/00268948108073573

Mol. Cryst. Liq. Cryst., 1981, Vol. 68, pp. 311–330
0026-8941/81/6801-0311 $06.50/0

Two Frequency Addressing of a DTN-Cell†

I. FUKUDA,‡ M. AKATSUKA,§ T. UCHIDA and M. WADA||

Department of Electronic Engineering, Faculty of Engineering, Tohoku University, Sendai 980, Japan

(*Received August 7, 1980; in final form September 29, 1980*)

The authors have already reported that a DTN-cell (depolarization in a twisted nematic-cell) had several advantages to a matrix display such as sharp threshold and wide viewing angle. But if the usual amplitude selection method is applied to a large scale matrix display using the DTN-mode, multiplex capability is limited by the cutoff frequency f_c of a liquid crystal. Therefore, the authors investigated a two frequency addressing method, that is, simultaneous application of a constant low-frequency voltage and a variable high-frequency voltage. In this method, a liquid crystal with lower-f_c can be used. In addition, some advantages of extremely sharp threshold, high contrast and relatively fast response and recovery can be obtained by using a liquid crystal with large negative dielectric anisotropy. These advantages are useful for a large scale matrix display.

1 INTRODUCTION

Liquid crystal display devices (LCDs) have been widely used because of their many advantages such as low power consumption, low driving voltage and flat panel structure. At present, the fields of their application are limited to displays of portable instruments with small scale information such as watches and calculators. As a recent trend of LCDs, however, researches and developments of a large scale matrix display are being done actively.[1~6] There are many technical difficulties for LCDs to be applied to a large scale matrix display, because LCDs generally have the following disadvantages to a large scale matrix display:

(1) The threshold sharpness is insufficient.

(2) Response and recovery are rather slow.

† Presented at the Eighth International Liquid Crystal Conference, Kyoto, July, 1980.
‡ Present address: Kanazawa Institute of Technology, Kanazawa 921, Japan.
§ Present address: Asahi Glass Corporation Ltd., Yokohama 221, Japan.
|| Passed away on January 10, 1980.

Therefore, various experiments to improve the multiplex capability have been made, combining the LCD with control devices such as a PLZT-ferroelectric layer[2] and a ZnO-varistor[3] or with active control devices such as a thin film transistor (TFT)[4] and a MOS-field effect transistor (MOS FET).[5,6] But their structures are complex and hence require much cost of production. Therefore, the simple matrix display without a nonlinear device or an active device is desirable.

Almost all LCDs put in practical use at present are twisted nematic type (abbreviated as TN-type)[7] among many suggested display modes. But this type has disadvantages of narrow viewing angle and the relatively insufficient multiplex capability when the usual driving technique of amplitude selection method is used. On the other hand, a depolarization in twisted nematic liquid crystal layer mode (abbreviated as DTN-mode)[8,9] suggested by the authors has a wide viewing angle and a sharp threshold though it has to be used as a transmissive display because of relatively poor brightness. Therefore, it is suitable for a large scale matrix display.

In this paper, multiplex capability of the DTN-cell is discussed and its problems are clarified. Then, it is stated that the problems can be solved by two frequency addressing method. In addition, various display characteristics of the cell driven by this method are discussed.

2 FUNDAMENTAL OPERATION OF THE DTN-CELL

The structure of the DTN-cell is schematically shown in Figure 1. A cell with two parallel glass plates, G_1 and G_2, is filled with a liquid crystal of negative dielectric anisotropy, which has twisted alignment of an angle 90°. Plates P_1 and P_2 are polarizers and D is a diffuser. The incident light is linearly polarized after passing through P_1. It then proceeds into the cell, in which the plane of polarization suffers a rotation of an angle 90° in passing through the glass plate G_2. The plane of polarization of the second polarizer P_2 is adjusted to be at right angles with its incident light when no voltage is applied to the cell, thereby allowing no transmission of light through the polarizer (Figure 2a). When a voltage is applied to the cell, electrohydrodynamic instability[10] occurs as shown in Figure 2b, which causes the light to be depolarized while passing through the cell. This produces the component of polarization that can pass P_2 and the device is converted to the bright state.

3 EXPERIMENTAL

Table I shows the liquid crystal and the additives used in this experiment. The nematic liquid crystals were a typical Schiff base mixture of MBBA 50wt%

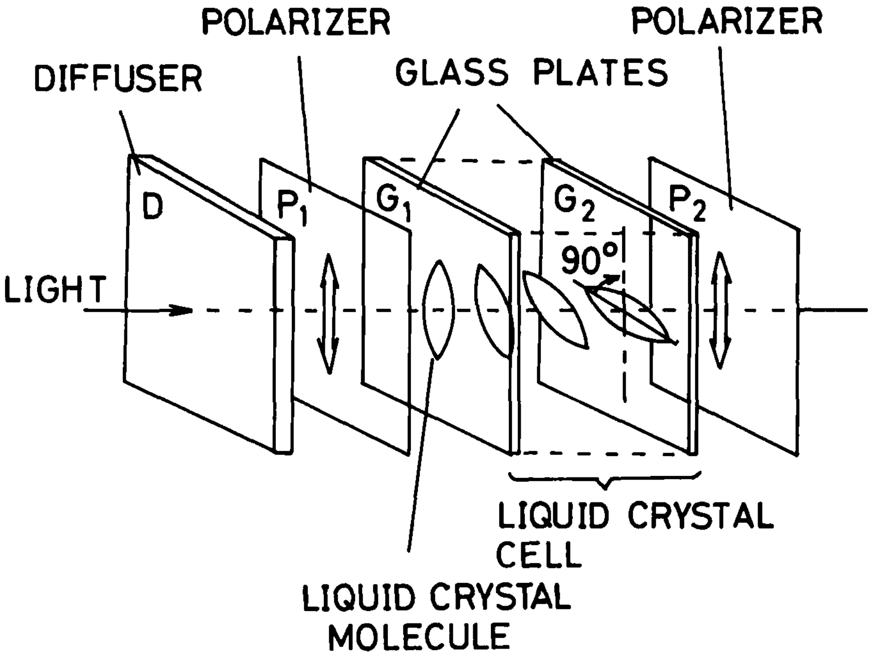

FIGURE 1 Structure of the DTN-cell.

and EBBA 50wt% with dielectric anisotropy $\Delta\epsilon$ of −0.45 and a ester mixture EN-18 of Chisso Corp. with large negative $\Delta\epsilon$ of −5.9. Both liquid crystals were doped with an ionic material, tetrabutylammonium bromide (TBAB), to increase the cutoff frequency f_c[11,12] of a liquid crystal to about 2 kHz. In addition, a small amount (about 0.03wt%) of a cholesteric liquid crystal was added to both mixtures to prevent reverse twisting. The liquid crystal cell was made of two In_2O_3 coated glass plates, whose surfaces were treated with N-β(aminoethyl)γ-aminopropyltrimethoxysilane (AAMS)[13] followed by unidirectional

TABLE I

The liquid crystals and additives used in the experiments

Host nematic liquid crystal	Additives	$\Delta\epsilon$	f_c (kHz)
$MBBA_{50}$ $EBBA_{50}$	TBAB, CC	−0.45	1.6
EN-18	TBAB, CC	−5.9	2.3

MBBA: *p*-methoxybenzylidene-*p'*-*n*-butylaniline.
EBBA: *p*-ethoxybenzylidene-*p'*-*n*-butylaniline.
EN-18: an ester mixture (produced by Chisso Corp. $\Delta\epsilon = -5.9$).
TBAB: tetrabutylammonium bromide.
CC: cholesteryl chloride.

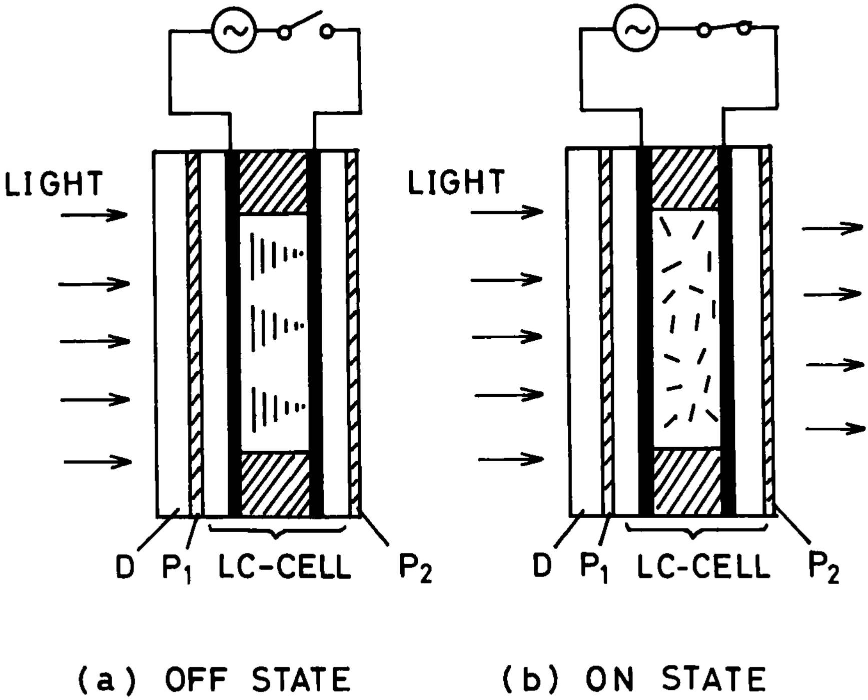

FIGURE 2 Liquid crystal orientation in the DTN-cell.

rubbing. By this surface treatment, liquid crystal molecules aligned unidirectionally parallel to the glass plates. Square wave voltages of 50 Hz and 10 kHz were respectively used for low-frequency and high-frequency voltage. All measurements were made at 25°C.

4 RESULTS AND DISCUSSION

4.1 Single frequency addressing of the DTN-cell

Figure 3 shows the typical basic characteristic of the DTN-cell when it is driven by a low-frequency voltage. As shown in this figure, the threshold voltage and the peak voltage are denoted by $V_{l,th}$ and V_p, respectively. When the usual addressing method of single frequency is applied to the matrix display of DTN-mode, the applied voltage to pixels is switched between voltages lower than $V_{l,\mathrm{th}}$ and higher than V_p by using the optimized amplitude selection method.[14,15] Table II shows a voltage waveform of the a:1 amplitude selection method. Figure 4 shows the typical waveforms applied to the on- or off-pixels. The rms-voltages for these on- and off-waveforms are expressed as

$$V_{\mathrm{on}} = \frac{V_0}{a}\sqrt{1 + \frac{a^2 - 1}{N}} \tag{1}$$

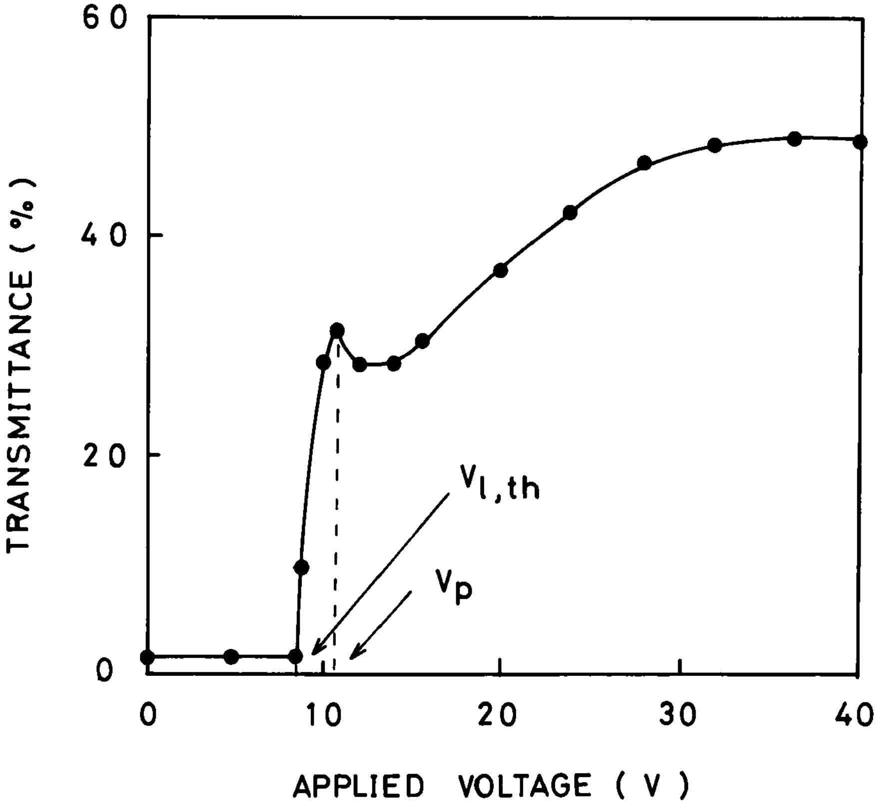

FIGURE 3 The fundamental characteristic of the DTN-cell.

$$V_{off} = \frac{V_0}{a}\sqrt{1 + \frac{(a-2)^2 - 1}{N}} \tag{2}$$

where N is the number of scanning electrodes and a is the bias constant. Here, if a is expressed as

$$a = \sqrt{N} + 1 \tag{3}$$

the ratio V_{on}/V_{off} becomes maximum and is expressed as

$$V_{on}/V_{off} = \sqrt{\frac{\sqrt{N}+1}{\sqrt{N}-1}} \tag{4}$$

This addressing method is called the optimized amplitude selection method. On the contrary, if the highest voltage of nonexcited state V_n and the lowest voltage of excited state V_e of a LCD are given, the maximum number of scan-

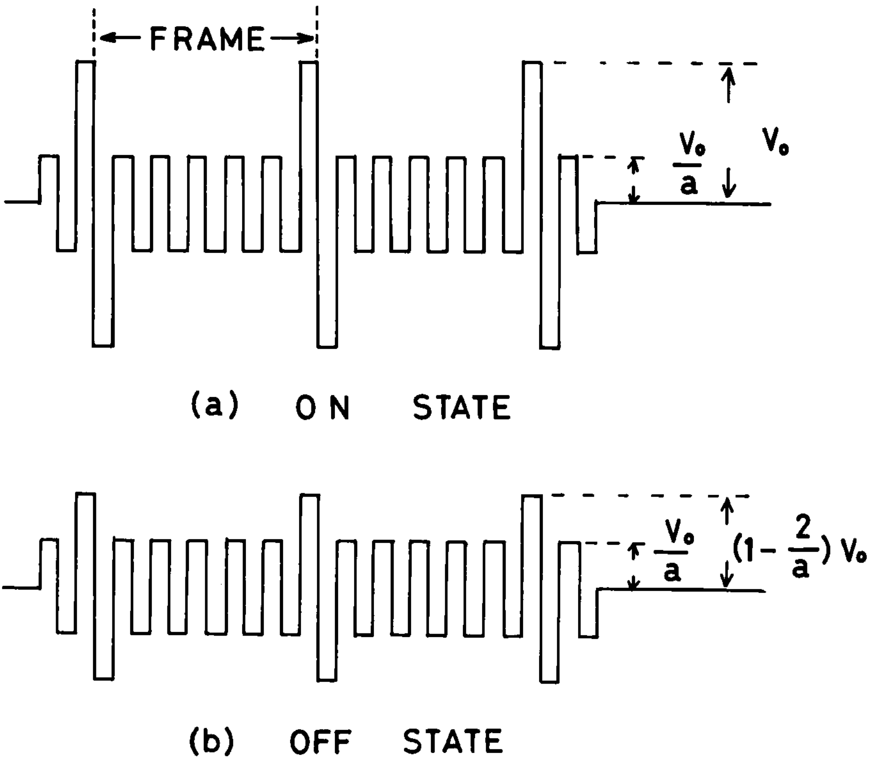

FIGURE 4 The waveforms of a:1 amplitude selection method.

ning electrodes N_m is expressed by substituting V_e/V_n for V_{on}/V_{off} in Eq. (4) as

$$N_m = \left(\frac{(V_e/V_n)^2 + 1}{(V_e/V_n)^2 - 1} \right)^2 \tag{5}$$

Figure 5 shows the relationships between V_e/V_n and N_m. In the case of the DTN-matrix cell, let V_n and V_e respectively correspond to $V_{l,th}$ and V_p. Then the maximum electrode number can be obtained by Eq. (5). Figure 6 shows the dependences of transmittance of the cells using $MBBA_{50}$ $EBBA_{50}$ and EN-18 on the applied voltage of 50 Hz. The thickness of liquid crystal layer of these cells (abbreviated as cell thickness) were respectively 12μm and 11μm, the difference was confirmed to be negligible. These results indicate that the cell using EN-18 with large negative $\Delta\epsilon$ has sharper threshold and higher transmittance than the cell using $MBBA_{50}$ $EBBA_{50}$.

If the usual amplitude selection method of a single frequency is applied to a large scale matrix display, however, the driving waveform includes high-frequency components as shown in Figure 4. For example, for a matrix display of 100:1 and of frame frequency 40 Hz, the main frequency component becomes

TABLE II

Voltage waveforms applied to pixels in amplitude selection method

X-electrode (scanning) \ Y-electrode (signal)		On	Off
		0, $\frac{1}{a}V_0$	0, $\frac{1}{a}V_0$
Select	0, $\left(1-\frac{1}{a}\right)V_0$	0, V_0	0, $\left(1-\frac{2}{a}\right)V_0$
Nonselect	0	0, $\frac{1}{a}V_0$	0, $\frac{1}{a}V_0$

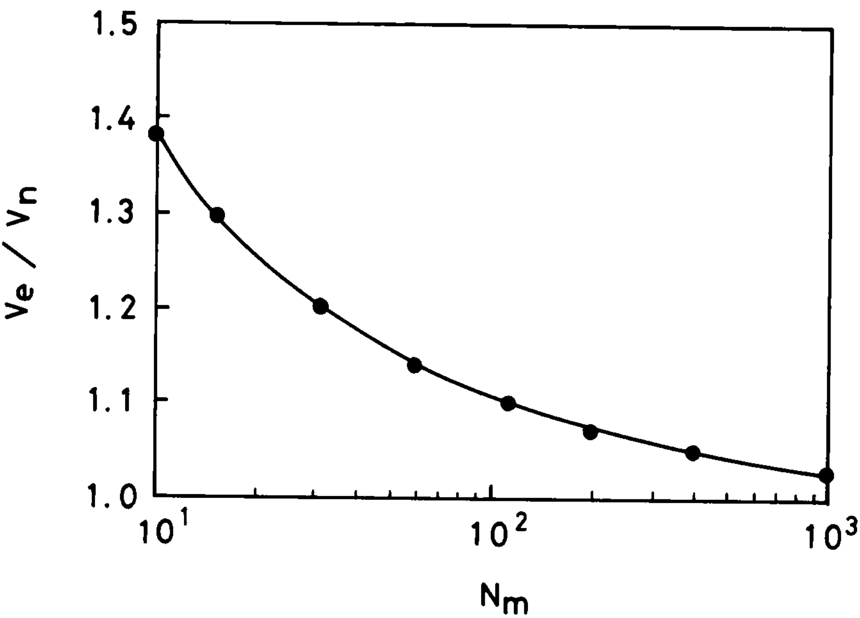

FIGURE 5 Relationship between the maximum number of scanning electrodes N_m and V_e/V_n.

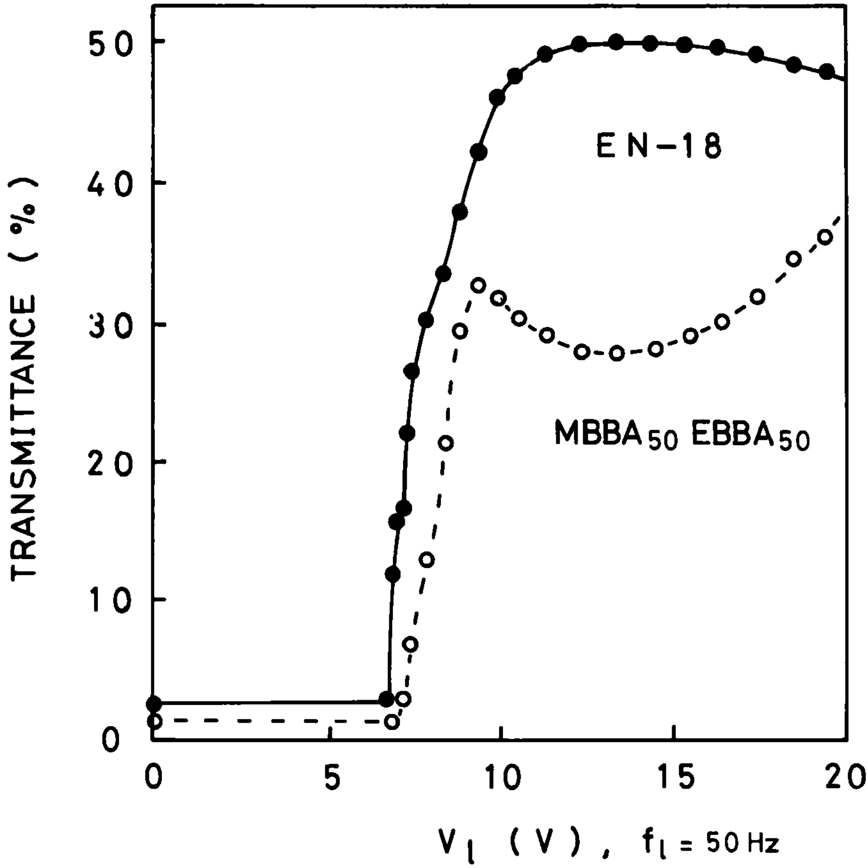

FIGURE 6 Dependences of transmittance of the cells using $MBBA_{50}$ $EBBA_{50}$ and EN-18 on the applied voltage of 50 Hz.

4 kHz. This indicates that the cutoff frequency f_c of a liquid crystal must be sufficiently higher than 4 kHz and hence heavy doping of an ionic compound is required. However, it seems to be disadvantageous in power consumption and electrochemical stability. In addition, when the number of scanning electrodes increases, V_{on}/V_{off} decreases and then response and recovery become slower. Therefore, we investigated the two frequency addressing of the DTN-cell to improve these problems. The results are shown in the next section.

4.2 Two frequency addressing of the DTN-cell

4.2.1 Addressing method The voltage of a frequency above f_c has the effect of suppressing the dynamic scattering. Two frequency addressing method of a dynamic scattering cell (abbreviated as DS-cell) utilizing this effect has already reported by C. R. Stein[16] and P. J. Wild *et al.*[17] However, their methods

TABLE III

Voltage waveforms applied to pixels in a high frequency addressing method

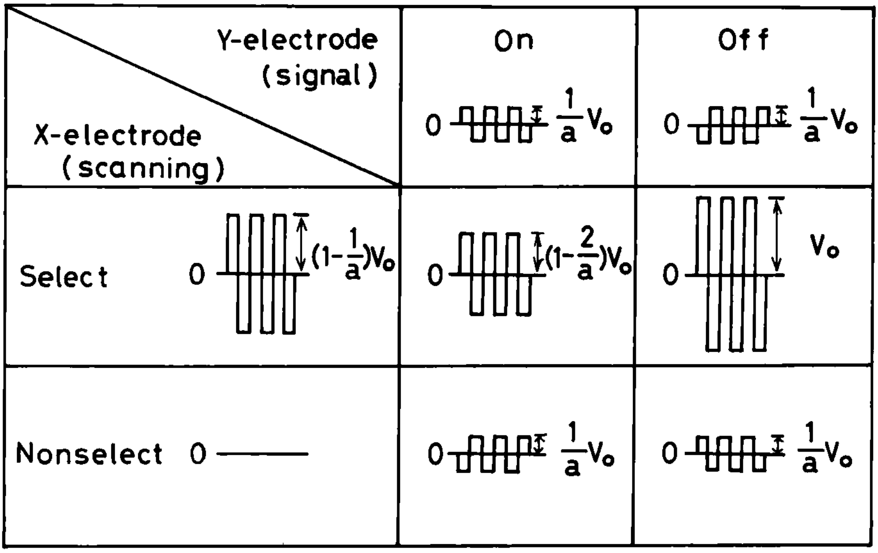

X-electrode (scanning) \ Y-electrode (signal)		On	Off
		0, $\frac{1}{a}V_0$	0, $\frac{1}{a}V_0$
Select	0, $(1-\frac{1}{a})V_0$	0, $(1-\frac{2}{a})V_0$	0, V_0
Nonselect	0	0, $\frac{1}{a}V_0$	0, $\frac{1}{a}V_0$

have the same problems as the single frequency addressing method in the point that a high f_c is required, because the low frequency voltage is also used for addressing. Therefore, the authors have investigated an improved two frequency addressing method for the DTN-cell, in which a constant low-frequency voltage and an addressing high-frequency voltage shown in Table III are simultaneously applied to the cell.[14] This method has an important advantage that the high f_c is not required for a large scale matrix display.

4.2.2 Electrooptical characteristics Figure 7(a) shows the low-frequency voltage dependence of the transmittance of the DTN-cell using $MBBA_{50}$ $EBBA_{50}$ where the frequency is 50 Hz. Figure 7(b) shows the characteristics of the same cell when it is driven by a variable high-frequency voltage (10 kHz) and a constant low-frequency voltage (50 Hz) corresponding to $a \sim d$ in Figure 7(a). This result indicates that relatively sharp threshold of high-frequency voltage can be obtained when V_l is adjusted to about $V_p(= 9.4V)$. By the way, for V_l larger than V_p, the transmittance near the high-frequency threshold voltage $V_{h,th}$ decreases and the recovery becomes slower. Therefore, in the case of $MBBA_{50}$ $EBBA_{50}$, the most preferable characteristics in the two frequency driving method can be obtained when V_l is adjusted to about V_p. Figure 8 shows the same characteristics using EN-18 with large negative $\Delta\epsilon$. In this case, an extremely sharp threshold of high frequency, a high transmittance and a large contrast ratio are obtained in comparison with the case of $MBBA_{50}$

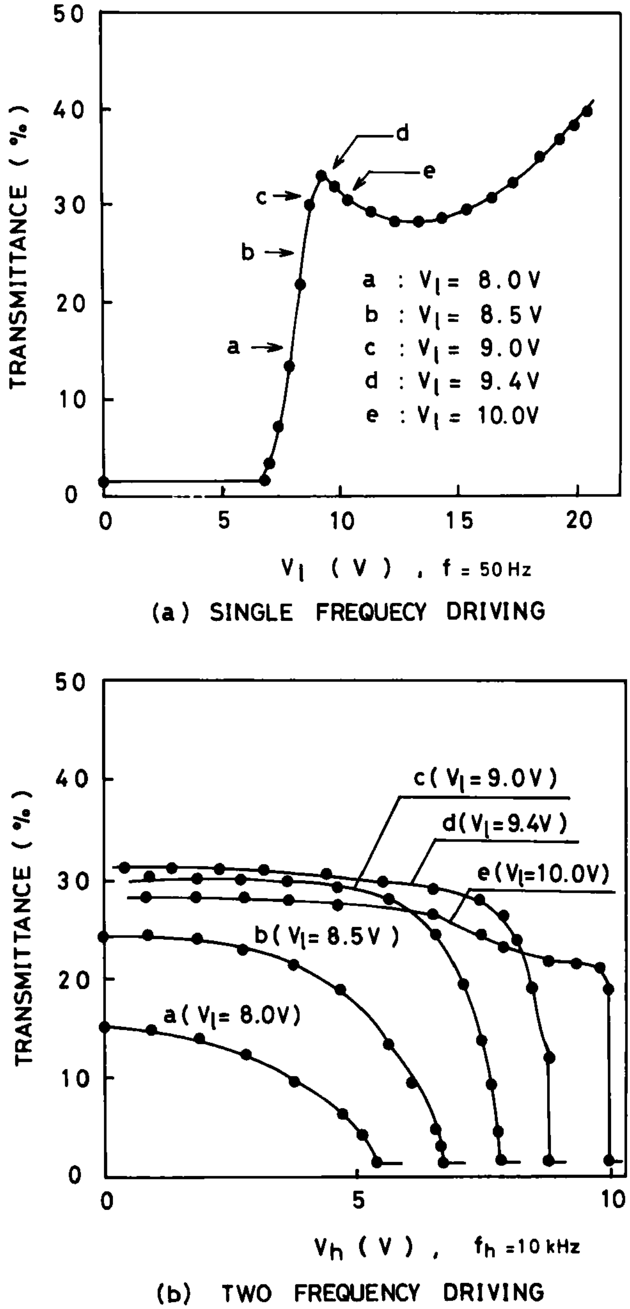

FIGURE 7 Applied voltage dependences of transmittance of the cell using $MBBA_{50}$ $EBBA_{50}$ (cell thickness: 11 μm).

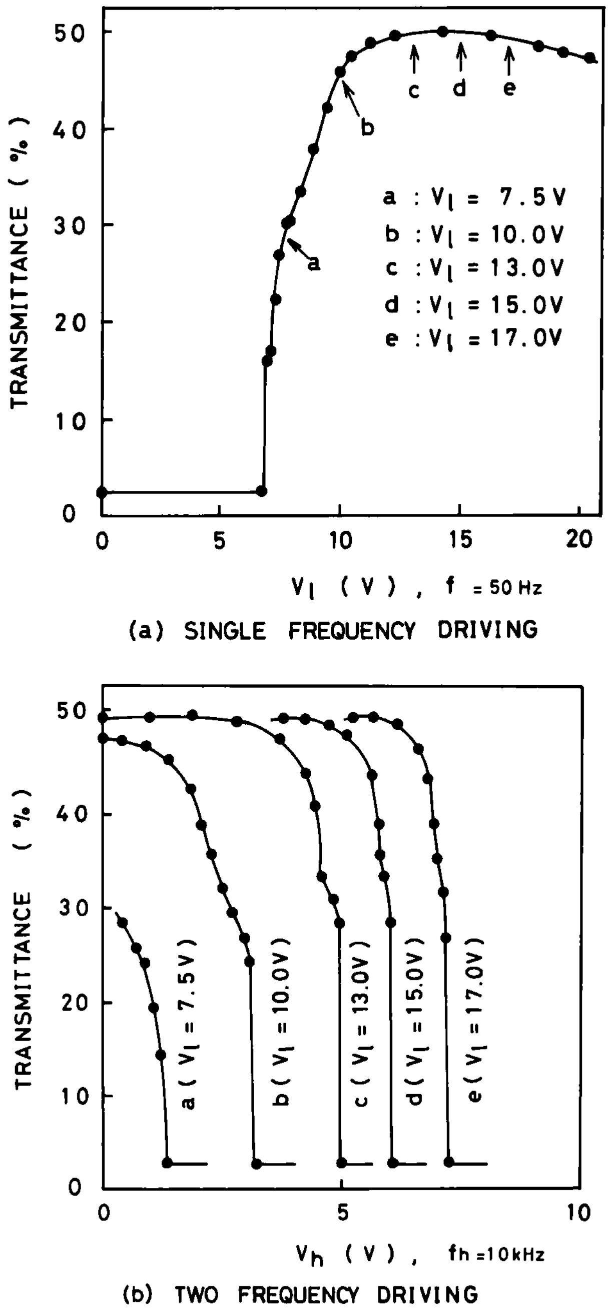

FIGURE 8 Applied voltage dependences of transmittance of the cell using EN-18 (cell thickness: 12μm).

$EBBA_{50}$. These characteristics are further improved by increasing V_l. As for the threshold voltage of high-frequency voltage, $V_{h,th}$, $MBBA_{50}$ $EBBA_{50}$ exhibits relatively high $V_{h,th}$ (8.3V) when V_l is adjusted to V_p (= 9.4V) which is the best condition in the two frequency driving method of this material. On the other hand, the threshold $V_{h,th}$ of EN-18 is fairly low (1.4V) when V_l is adjusted to 7.5V which corresponds to V_p. In the case of EN-18, however, contrast ratio, response and recovery times are further improved by increasing V_l to 10 ~ 15V, still $V_{h,th}$ is lower than that of $MBBA_{50}$ $EBBA_{50}$. For example, when V_l is 10V, 13V, 15V, $V_{h,th}$ becomes 3.1V, 5.0V, 6.1V, respectively.

It is difficult to produce a uniform thickness of liquid crystal layer t, or cell thickness, when a large display device is produced. Therefore, it is desirable that the display characteristics are almost independent of the thickness. Figure 9 shows the effect of cell thickness on characteristics of the cell using EN-18

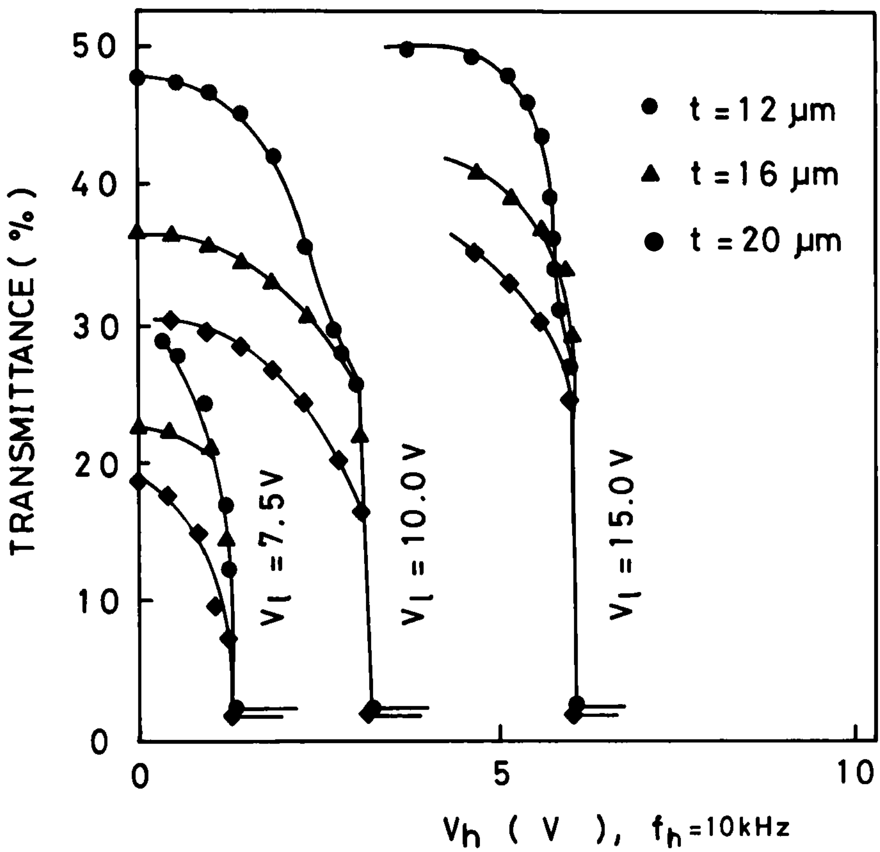

FIGURE 9 Effect of cell thickness on characteristics of the DTN-cell using EN-18 driven by two frequency voltages.

driven by two frequency voltages. These results indicated that $V_{h,\mathrm{th}}$ is almost independent of the thickness though the transmittance near the threshold decreases with increase of the cell thickness.

When a DS-cell is driven by the simultaneous application of two frequency voltages, V_l and V_h, whose frequency f_l and f_h are respectively $f_l \ll f_c$ and $f_h \gg f_c$, the relationship between V_l and V_h at the threshold is known to be expressed as[16,17]

$$V_l^2 = V_{l,\mathrm{th}}^2 + \gamma V_{h,\mathrm{th}}^2 \qquad (6)$$

where $V_{l,\mathrm{th}}$ is the threshold voltage of low frequency and γ is a coefficient dependent upon several material properties such as dielectric constant, viscosity and conductivity. The value of γ of the typical liquid crystal MBBA has been reported to be 0.5 at 32°C.[16] Figure 10 shows the relationships between V_l^2 and $V_{h,\mathrm{th}}^2$ of the DTN-cells using $MBBA_{50}$ $EBBA_{50}$ and EN-18. The relation for EN-18 is not linear and hence γ depends on V_l as shown in Figure 11, the reason of which is not clarified yet. It is shown that EN-18 has γ about ten times larger than that of $MBBA_{50}$ $EBBA_{50}$. This indicates that the suppressing effect of high-frequency voltage in EN-18 is very strong because of a large negative $\Delta\epsilon$.

4.2.3 Response and recovery properties Figure 12 shows the typical characteristic of the DTN-cell using EN-18 when it is driven by a variable high-fre-

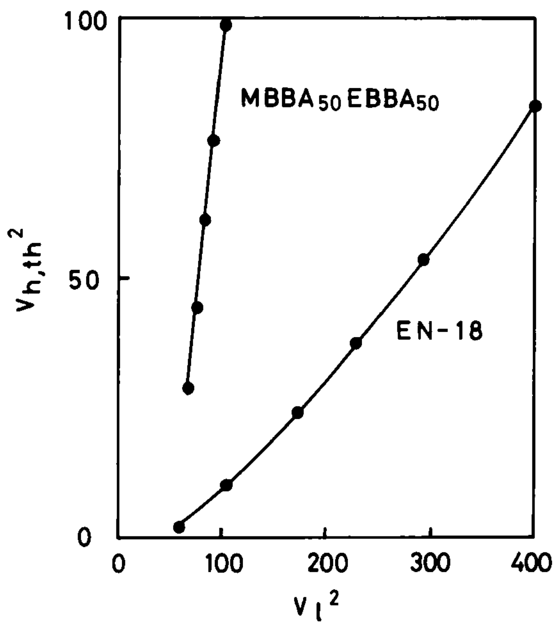

FIGURE 10 Relationships between V_l^2 and $V_{h,\mathrm{th}}^2$ in the cells using $MBBA_{50}$ $EBBA_{50}$ and EN-18.

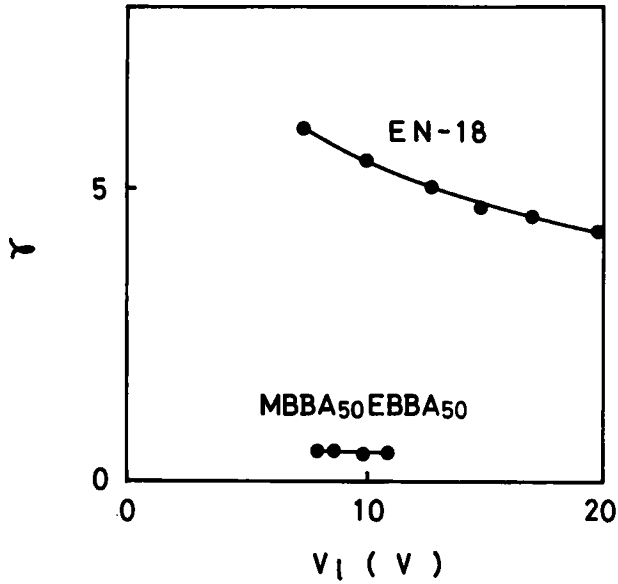

FIGURE 11 V_l dependences of γ in the cells using $MBBA_{50}$ $EBBA_{50}$ and EN-18.

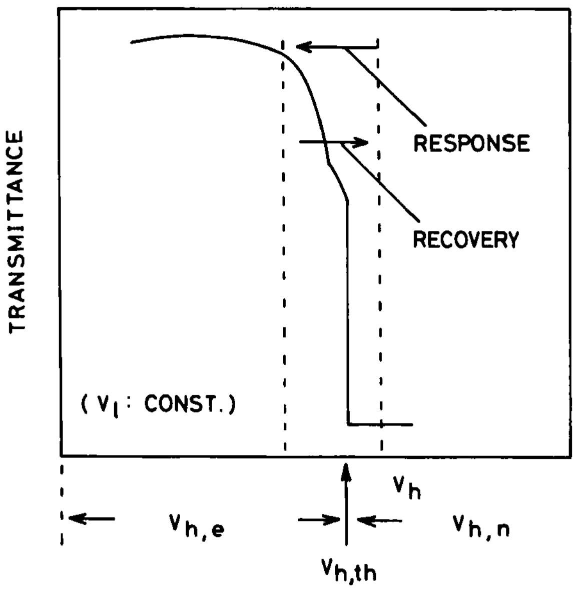

FIGURE 12 The fundamental characteristic of two frequency driving of the DTN-cell using EN-18 (V_h: a variable high-frequency voltage, V_l: a constant low-frequency voltage).

quency voltage V_h and a constant low-frequency voltage V_l. The cell becomes excited state at $V_h < V_{h,\text{th}}$ and nonexcited state at $V_h > V_{h,\text{th}}$. Then, voltages correspond to these states are denoted by $V_{h,n}$ and $V_{h,e}$ respectively. When the cell is driven by the two frequency voltages, V_h is switched from $V_{h,n}$ to $V_{h,e}$ (response) or from $V_{h,e}$ to $V_{h,n}$ (recovery) according to display signals. Therefore, response and recovery times under switching between $V_{h,e}$ and $V_{h,n}$ are important. In the case of a large scale matrix display, it is desirable to take $V_{h,n}$ as close to $V_{h,\text{th}}$ as possible for increasing the scanning electrodes and contrast ratio. Figure 13(a) and (b) shows $V_{h,e}$ dependence of response and recovery times for various V_l values, where $V_{h,n}$ is adjusted to 1.01 $V_{h,\text{th}}$. These results are summarized as follows.

(1) The response time depends on V_l and $V_{h,e}$. Namely, it becomes shorter as V_l increases and as $V_{h,e}$ decreases.

(2) The recovery time is almost independent of V_l and $V_{h,e}$.

(3) When V_l is adjusted to a fairly large value, relatively fast response and recovery times can be obtained even if $V_{h,e}/V_{h,n}$ is close to 1.

Figure 14 shows $V_{h,n}$ dependence of response and recovery times for various values of $V_{h,e}$ when V_l is adjusted to 15V. This result indicates that response and recovery times are almost independent of $V_{h,n}$. It is found from these results that the characteristics shown in Figure 13(a) are important when the DTN-cell is driven by the two frequency voltages. Namely, relatively fast response can be obtained by adjusting V_l to as large value as possible, $V_{h,n}$ to a slightly larger than $V_{h,\text{th}}$, and $V_{h,e}$ to as small value as possible, while recovery time is almost independent of driving condition.

4.2.4 The multiplexability of the DTN-cell On the basis of the experimental results mentioned above, the multiplex capability of the DTN-cell using EN-18 driven by two frequency addressing method will be discussed. When $V_{h,e}$ and $V_{h,n}$ is decided, the number of scanning electrodes can be obtained by substituting $V_{h,n}/V_{h,e}$ into V_e/V_n in Eq. (5). For example, Eq. (5) and Figure 5 indicate that the matrix display with more than 100 electrodes requires $V_{h,n}/V_{h,e} \leqq 1.10$. Figure 15 shows the relationship between contrast ratio and the number of scanning electrodes in comparison with the case of single frequency addressing. It is seen that contrast ratio larger than 10:1 can be obtained by the two frequency addressing method with $V_l = 15$V even if the scanning electrodes number is 1000. Figure 16 shows the relationships between response and recovery times and the number of scanning electrodes. This result indicates that response time is about 140 msec and recovery time is about 220 msec when 200 electrodes are scanned at $V_l = 15$V. These values seem to be satisfying to a certain extent for practical use. Figure 17 shows the relationship between addressing peak voltage V_0 and the number of scanning electrodes. This

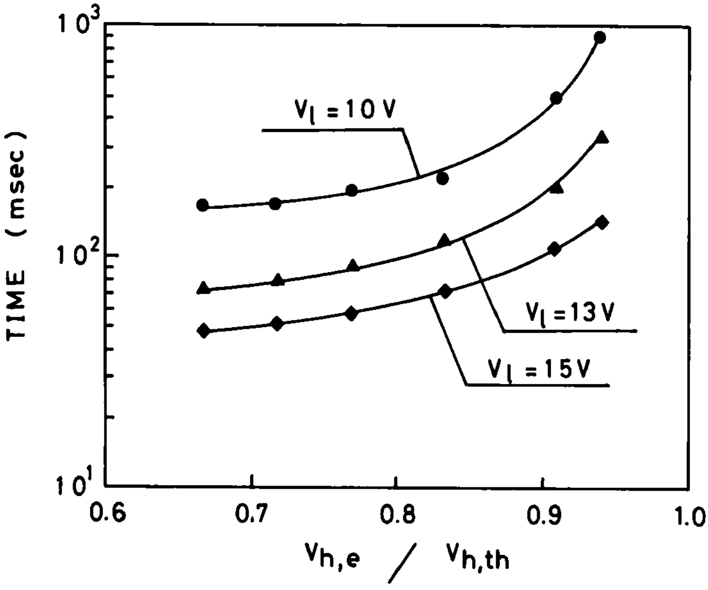

(a) RESPONSE

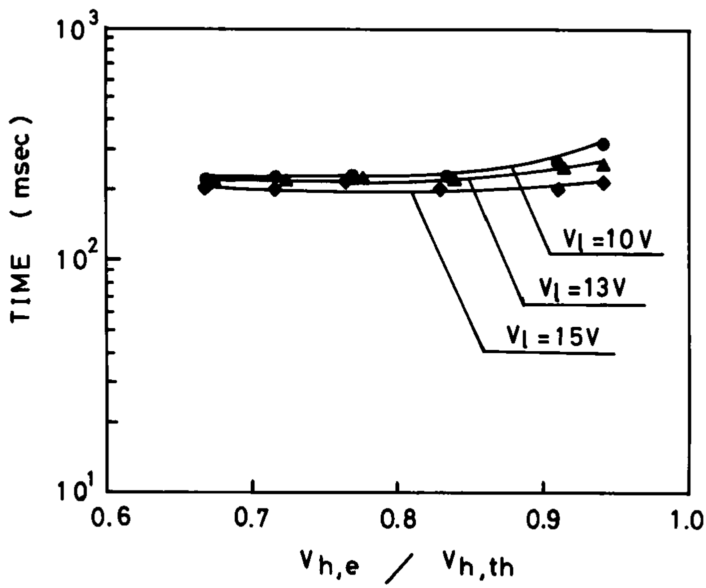

(b) RECOVERY

FIGURE 13 $V_{h,e}/V_{h,\text{th}}$ dependences of response and recovery times (liquid crystal: EN-18, cell thickness: 12μm, $V_{h,n} = 1.01\ V_{h,\text{th}}$).

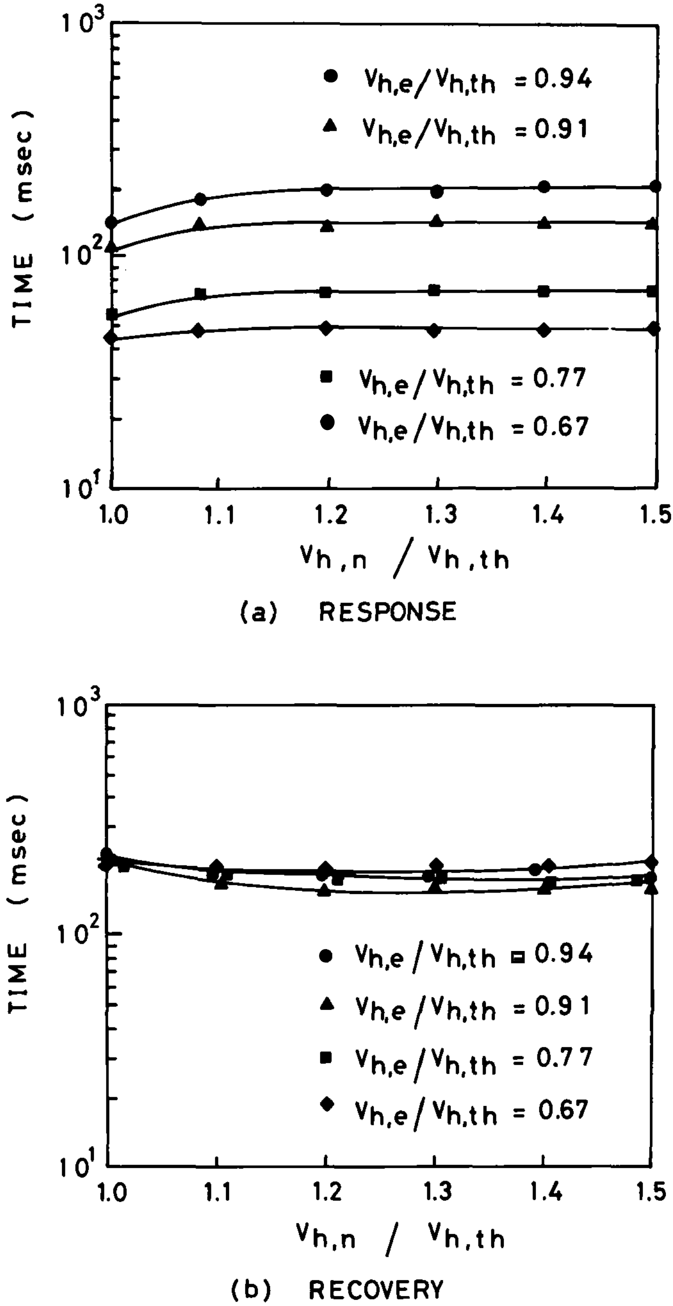

FIGURE 14 $V_{h,n}/V_{h,th}$ dependences of response and recovery times (liquid crystal: EN-18, cell thickness: 12μm).

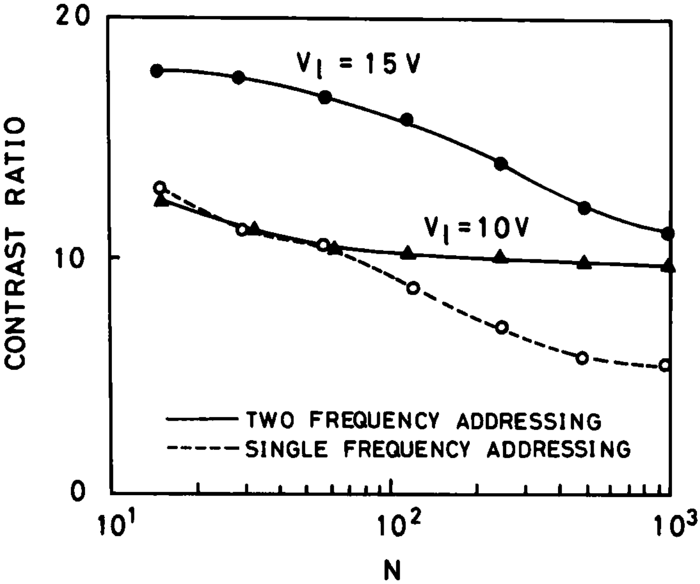

FIGURE 15 Relationships between contrast ratio and number of scanning electrodes N (liquid crystal: EN-18, cell thickness: 12μm).

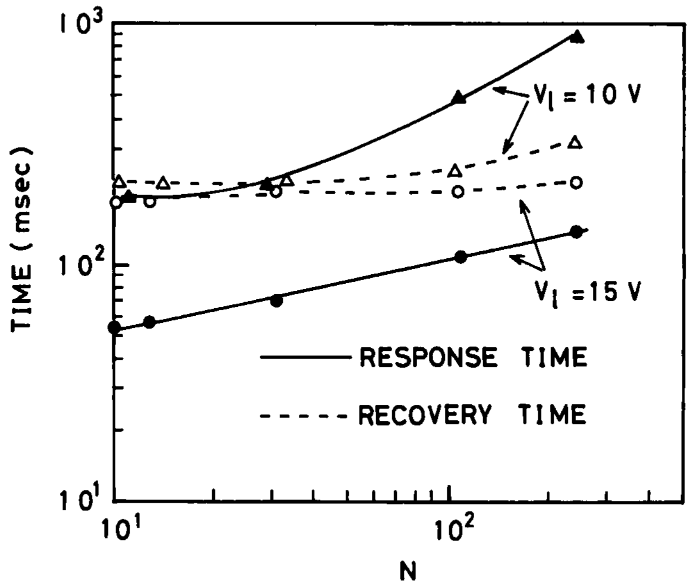

FIGURE 16 Relationships between response and recovery times and number of scanning electrodes N (liquid crystal: EN-18, cell thickness: 12μm).

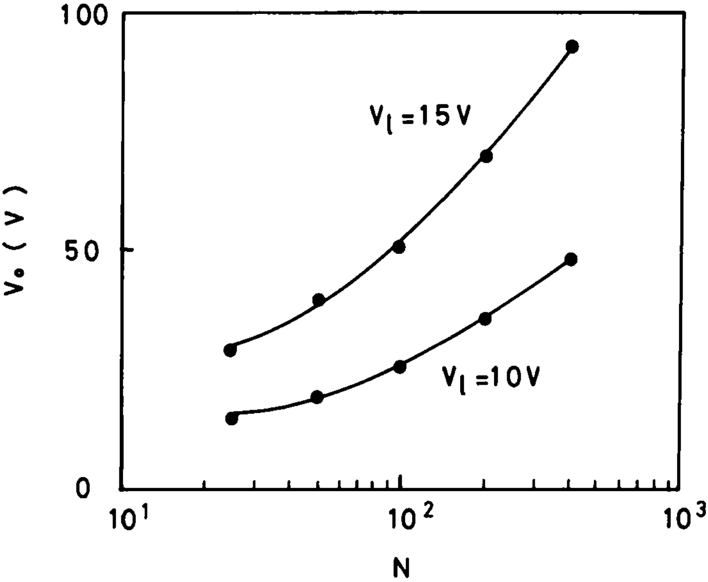

FIGURE 17 Relationships between addressing peak voltage V_0 and number of scanning electrodes N (liquid crystal: EN-18, cell thickness: 12μm).

indicates that a large scale matrix display can be driven by a relatively low voltage when V_l is adjusted about 10V. However, response time increases in the case of a large number of scanning electrodes. On the other hand, when V_l is adjusted to about 15V, contrast ratio and response time are improved but V_0 becomes relatively high. For example, it becomes about ±50V and ±70V for 100 and 200 scanning electrodes respectively. However, it may be possible to reduce the addressing voltage if the liquid crystal with larger negative $\Delta\epsilon$ will be developed.

5 CONCLUSION

When the DTN-cell using a liquid crystal with large negative dielectric anisotropy is driven by the two frequency addressing method, in which a constant low-frequency voltage and a high-frequency addressing voltage simultaneously applied, the following advantages to a large scale matrix display can be obtained.

(1) Extremely sharp threshold of high-frequency voltage can be obtained.

(2) High transmittance and high contrast can be obtained.

(3) Relatively fast response and recovery can be obtained.

TABLE IV

The multiplexability of the DTN-cell (liquid crystal: EN-18, cell-thickness: 12 μm, V_l = 15V)

Number of scanning electrodes N	Contrast ratio	Response time (msec)	Recovery time (msec)	Addressing peak voltage V_o (V)
100	1:16	110	200	±50
200	1:14	140	220	±70

(4) High-frequency threshold voltage $V_{h,th}$ is independent of cell thickness.

(5) Viewing angle is very wide.

(6) High-f_c is not required.

As a result, the multiplexability as shown in Table IV can be obtained. If a liquid crystal with larger negative $\Delta\epsilon$ is developed, the addressing voltage will be more decreased.

Acknowledgments

The authors would like to express their hearty thanks to Professor Y. Shibata for his helpful advice. They are also deeply indebted to Miss C. Shishido, Dr. H. Seki, Mr. M. Ohgawara and Mr. Y. Takahashi for their kindly assistance.

This work was financially supported by the Grant-in-Aid for Scientific Research from the Ministry of Education Science and Culture of Japan.

References

1. K. Odawara, T. Ishibashi, K. Kinugawa, H. Sakurada and H. Tanaka, *Proc. SID*, **21**, 79 (1980).
2. L. E. Tannas, Jr. and P. K. York, SID 1973 Symp. Digest, 178.
3. D. E. Castleberry, *IEEE Trans. Electron Devices*, **ED-26**, 1123 (1979).
4. T. P. Brody, J. A. Asars and G. D. Dixon, *IEEE Trans. Electron Devices*, **ED-20**, 995 (1973).
5. L. T. Lipton, C. P. Stephens, R. B. Lloyd, S. E. Shields, A. G. Toth and R. C. Tsai, SID 1978 Symp. Digest, 96.
6. M. Yoshiyama, T. Matsuo, K. Kawasaki, H. Tatsuta and H. Irie, *National Technical Report*, **25**, 500 (1979).
7. M. Schadt and W. Helfrich, *Appl. Phys. Lett.*, **18**, 127 (1971).
8. T. Uchida, Y. Ishii and M. Wada, *IEEE Trans. Electron Devices*, **ED-26**, 1375 (1979).
9. T. Uchida, Y. Ishii and M. Wada, *Proc. SID*, **21**, 55 (1980).
10. W. Helfrich, *J. Chem. Phys.*, **51**, 4092 (1969).
11. E. D. Violette, P. G. de Gennes and O. Parodi, *J. Phys.*, **32**, 305 (1971).
12. Orsay Liquid Crystal Group, *Mol. Cryst. Liq. Cryst.*, **12**, 251 (1971).
13. T. Uchida, K. Ishikawa and M. Wada, *Trans. Inst. Elec. Commun. Eng. Japan*, **61**, 289 (1978).
14. P. M. Alt and P. Pleshko, *IEEE Trans. Electron Devices*, **ED-21**, 146 (1974).
15. H. Kawakami and Y. Yoneda, Tech. Group on Image Eng., Inst. Electron. Commun. Eng. Japan, Paper IE73-46 (1974).
16. C. R. Stein and R. A. Kashnow, *Appl. Phys. Lett.*, **19**, 343 (1971).
17. P. J. Wild and J. Nehring, *Appl. Phys. Lett.*, **19**, 335 (1971).